Viscosity-modulated breakup and coalescence of large drops in bounded turbulence

Alessio Roccon

Inst. of Fluid Mechanics and Heat Transfer
TU Wien
1060 Wien, Austria
alessio.roccon@tuwien.ac.at

Francesco Zonta

Inst. of Fluid Mechanics and Heat Transfer
TU Wien
1060 Wien, Austria
francesco.zonta@tuwien.ac.at

Alfredo Soldati

Inst. of Fluid Mechanics and Heat Transfer
TU Wien
1060 Wien, Austria
alfredo.soldati@tuwien.ac.at

ABSTRACT

In this work, we examine the influence of viscosity on breakup and coalescence of a swarm of large drops in a wall-bounded turbulent flow. We consider several values of surface tension and a wide range of drops to fluid viscosity ratios $\lambda = \eta_d/\eta_c$ (with η_d the viscosity of drops and η_c the viscosity of the carrier fluid), from $\lambda = 0.01$ to $\lambda = 100$, while we maintain the same density for drops and carrier fluids. Drops can coalesce and break following a complex dynamics that is primarily controlled by the interplay between turbulence fluctuations (measured by Re_τ), surface tension (measured by We) and λ. We use Direct Numerical Simulations (DNS) of turbulence coupled with a Phase Field Method (PFM) to describe the drops dynamics. We consider three different values of We (which is the inverse of the surface tension): $We = 0.75$, $We = 1.5$ and $We = 3$. For each value of We, we assume five values of λ: $\lambda = 0.01$, $\lambda = 0.10$, $\lambda = 1.00$, $\lambda = 10.0$ and $\lambda = 100$. We observe a consistent action of increasing λ, which, especially for the larger Weber numbers decreases significantly the breakup rate of the drops. Qualitatively, an increase of drop viscosity decreases the breakup rate, very much like an increase of surface tension does. The mechanism by which drop viscosity acts is a modulation of turbulence fluctuations inside the drop, which reduces the work surface tension has to do to preserve drop integrity. We believe that this may give important indications in many industrial applications to control drop coalescence and fragmentation via the ratio of drop-to-fluid viscosity.

INTRODUCTION

Prediction of breakup and coalescence rates of a swarm of liquid drops immersed in a turbulent liquid flow (liquid/liquid emulsion) is crucially dependent on a number of hard-to-tackle factors. Among many others these include turbulence, turbulence/interface interactions, surface tension effects and viscosity gradients. Each single of these effects has a specific action on breakup and coalescence, and we can envision drops dynamics as the ultimate result of a complex competition between destabilizing and stabilizing effects. Destabilizing effects are primarily due to the combined effects of fluctuating inertial and shear terms acting at the drops interface. Stabilizing effects are due to surface tension, which is a restoring force acting to preserve drops sphericity. The outcome of this competition determines drops deformation, breakage and coalescence. In this picture, viscosity gradients across the interface of the drops can act as modulators of the localized shear stresses and can amplify or damp the initial turbulence perturbations to the point of changing profoundly the final result. Drops coalescence and breakup is of paramount importance in many environmental and industrial applications, from transport of pollutant drops in water bodies (Wu *et al.* (2010)) to hydrocarbon separation or oil-water emulsions in chemical plants and petroleum industry (Joseph *et al.* (1984); Chen *et al.* (1990); Ahmadi *et al.* (in press)). In this paper we focus precisely on liquid-liquid emulsions, in which drops of one phase are dispersed within the other phase. In this instance, the knowledge of the drops number density and/or the drops interface extension is a key parameter to optimize the design of efficient oil separators, in which drops coalescence should be promoted and drops fragmentation reduced. For drops breakup in turbulence, literature dates back to the seminal work of (Hinze (1955)), who modelled the mechanism of liquid drops splitting in a turbulent gas environment. Since the fundamental physics of drops splitting in gas-liquid or liquid-liquid configurations is controlled by the same parameters, results obtained for the gas-liquid case have been historically (and successfully) applied to the liquid-liquid case as well. In accordance with (Hinze (1955)), drop breakup occurs when the Weber number We, (i.e. the ratio between inertia and surface tension) exceeds a critical value, We_{cr}. Assuming a drop size in the inertial range of turbulence (so that Kolmogorov's law can be used to define turbulence fluctuations at the drop scale), (Hinze (1955)) was able to predict the maximum size of a drop that will not be broken by turbulence in a given flow. Based on available experimental data (Clay (1940*a*,*b*); Hinze (1955)) finally proposed $We_{cr} = 1.18$, even though a general agreement on the value of We_{cr} is still to be found (the value of We_{cr} ranges between 1 and 12, largely depending on the employed fluids and on the flow configuration). Many subsequent theoretical and experimental studies (see Chen & Middleman (1967); Wang & Calabrese (1986*a*,*b*); Sleicher (1962); Collins & Knudsen (1970), among others) have been performed on drops size distribution in engineering-relevant situations (liquid-liquid emulsions in pipelines and stirred tanks), with most of these studies conducted in dilute conditions, so to neglect drops coalescence. However, in any practical situation, drops breakup and coalescence occur simultaneously and cannot be neglected when a complete characterization of the drop swarm dynamics is required (Shinnar (1961)). Unlike the case of drops breakup, drops coalescence has been the subject of relatively fewer studies, most of which

focused on the binary collision of two separate drops in still fluid (Qian & Law (1997); Ashgriz & Poo (1990); Paulsen *et al.* (2014)). Although these studies have definitely provided useful insights to understand the fundamental physics of drops collisions and merging, their extension to more complex situations like drops moving inside turbulent pipes or reactors is not straightforward and still requires a leap forward (Howarth (1964)). From the previous literature survey it is apparent that a large proportion of the work on drops breakup and coalescence is based on experimental or theoretical approaches. This is due to the complex nature of drops interactions that has hindered the development of accurate numerical simulations of the phenomenon. Only recently, numerics has become available to analyze complex multiphase flows situations. Accurate numerical simulations can help providing the time evolution of the drops deformation together with the description of the entire flow field inside and outside of the drop. This is extremely important for unsteady turbulent flow conditions, where it is essential to record the coupled drops/turbulence interactions in time and space. To the best of our knowledge, there are only few available Direct Numerical Simulations (Qian *et al.* (2006); Perlekar *et al.* (2012); Scarbolo *et al.* (2015); Komrakova *et al.* (2015); Skartlien *et al.* (2013)) of the collective drop dynamics in turbulence, none of which, however, consideres the case of fluids with different viscosities in wall-bounded turbulence. The aim of the present study is to extend available literature results on collective drops dynamics in wall-bounded turbulence considering the case of fluids with the same density but different viscosity. In particular, we will consider a wide range of drops-to-fluid viscosity ratio $\lambda = \eta_d/\eta_c$ (with η_d the viscosity of drops and η_c the viscosity of the carrier fluid), from $\lambda = 0.01$ to $\lambda = 100$. This paper is organized as follows. We will first describe the physical and numerical modelling used to perform the present simulations. Then, we will present and discuss our numerical results, focusing in particular on the role of drops surface tension and drops viscosity on their coalescence and breakup efficiency.

METHODOLOGY

We consider a two-phase flow system composed by large drops with density ρ_d and dynamic viscosity η_d dispersed in a turbulent channel flow (with the carrier fluid being characterized by density ρ_c and dynamic viscosity η_c). The origin of the reference frame is located at the center of the channel and the $x-$, $y-$ and $z-$axes point in the streamwise, spanwise and wall normal direction, respectively. The evolution of the two-phase flow system is described by a Phase Field Method (PFM), which in the recent years has been applied to this type of problems (Scarbolo *et al.* (2013, 2015)). The method is based on the use of a single variable ϕ (order parameter) to describe the entire binary system: ϕ is uniform in the bulk fluid regions ($\phi = \phi_+$ inside a drop and $\phi = \phi_-$ inside the carrier flow) and changes smoothly across the fluid-fluid interface. All the thermophysical properties of the fluids are proportional to the order parameter. The time evolution of the order parameter ϕ is described by the convective Cahn-Hilliard equation Anderson *et al.* (1998):

$$\frac{\partial \phi}{\partial t} = -\mathbf{u}\cdot\nabla\phi + \mathscr{M}\nabla^2\mu \tag{1}$$

where $\mathbf{u}$ is the velocity field, $\mathscr{M}$ is the mobility parameter driving the interface relaxation and μ is the chemical potential controlling the behaviour of the interfacial layer and defined in terms of a Ginzburg-Landau free energy functional:

$$\mathscr{F}[\phi,\nabla\phi] = \int_\Omega (f_0(\phi) + \frac{1}{2}\kappa|\nabla\phi|^2)d\Omega \tag{2}$$

The above expression of $\mathscr{F}[\phi,\nabla\phi]$, which is the sum of two different contributions, is used here to represent an immiscible binary mixture of isothermal fluids. In particular, $f_0(\phi)$ is the so-called double-well potential,

$$f_0(\phi) = \frac{\alpha}{4}\left(\phi_- + \sqrt{\frac{\beta}{\alpha}}\right)^2\left(\phi_+ - \sqrt{\frac{\beta}{\alpha}}\right)^2 \tag{3}$$

which accounts for the tendency of the system to separate into the two pure stable phases. The second term, $\frac{1}{2}\kappa|\nabla\phi|^2$ in Eq. (2), is a non-local term (mixing energy) accounting for the energy stored in the interfacial layer. Note that α and β are two positive constants that define the interface properties, whereas κ is a positive parameter used to describe the magnitude of the surface tension. The time evolution of the order parameter ϕ is driven by the minimization of $\mathscr{F}[\phi,\nabla\phi]$ (i.e by the chemical potential μ)

$$\mu = \frac{\delta\mathscr{F}[\phi,\nabla\phi]}{\delta\phi} = \alpha\phi^3 - \beta\phi - \kappa\nabla^2\phi \tag{4}$$

The Cahn-Hiliard equation (7) can be coupled with Navier-Stokes (6) and continuity equations to form a model for the computation of a multiphase flow (Jacqmin (1999); Yue *et al.* (2004); Badalassi *et al.* (2003)). Using the half channel height h as reference length, the shear velocity $u_\tau = \sqrt{\tau_w/\rho_c}$ (with τ_w the shear stress at the wall) as reference velocity, and the bulk value $\phi_+ = \sqrt{\beta/\alpha}$ as reference value of the order parameter, all the equations can be made dimensionless (with the superscript '+' indicating dimensionless variables being dropped for ease of reading) and the resulting set of equations is:

$$\nabla\cdot\mathbf{u} = 0 \tag{5}$$

$$\frac{\partial\mathbf{u}}{\partial t} + \mathbf{u}\cdot\nabla\mathbf{u} = -\nabla p + \frac{1}{Re_\tau}\nabla\cdot(\overline{\eta}(\nabla\mathbf{u} + \nabla\mathbf{u}^{\mathbf{T}})) + \frac{3}{\sqrt{8}}\frac{Ch}{We}\nabla\cdot\tau_{\mathbf{c}} \tag{6}$$

$$\frac{\partial\phi}{\partial t} + \mathbf{u}\cdot\nabla\phi = \frac{1}{Pe}\nabla^2\mu \tag{7}$$

where the term $\frac{3}{\sqrt{8}}\frac{Ch}{We}\nabla\cdot\tau_{\mathbf{c}}$ represents the capillary force due to surface tension ($\tau_{\mathbf{c}} = |\nabla\phi|^2\mathbf{I} - \nabla\phi\otimes\nabla\phi$ being the Korteweg stress), the gradient pressure can be decomposed as $\nabla p = \nabla p' + \Pi$, where the last term is the mean pressure gradient that drives the flow in the streamwise direction (kept constant during all the computation) and the function $\overline{\eta}(\phi,\lambda)$ accounts for the viscosity variations between the two phases. Note that the Ginzburg-Landau free energy potential $\mathscr{F}[\phi,\nabla\phi]$ and the chemical potential μ in dimensionless form become:

$$\mathscr{F}[\phi,\nabla\phi] = \frac{1}{4}(\phi-1)^2(\phi+1)^2 + \frac{1}{2}Ch^2|\nabla\phi|^2 \tag{8}$$

$$\mu = \phi^3 - \phi - Ch^2\nabla^2\phi \tag{9}$$

The dimensionless groups in Eqs. (7)-(6) are defined as:

$$Re_\tau = \frac{\rho u_\tau h}{\eta_c} \quad Pe = \frac{u_\tau h}{\mathscr{M}} \quad We = \frac{\rho u_\tau^2 h}{\sigma} \quad Ch = \frac{\xi}{h} \quad \lambda = \frac{\eta_d}{\eta_c} \tag{10}$$

From a physical point of view, Re_τ (shear Reynolds number) is the ratio between inertial and viscous forces whereas *We* is the ratio between inertial and surface tension forces. Note that increasing *We* increases the drops deformation (for $We \to 0$ drops behave like rigid spheres). The Peclet number *Pe* is the ratio between diffusive and convective time scales of the interface, while the Cahn number *Ch* is the dimensionless thickness of the interface. The Cahn-Hilliard (6) and Navier-Stokes (7) equations are coupled through the capillary term, $\frac{3}{\sqrt{8}}\frac{Ch}{We}\nabla \cdot \tau_{\mathbf{c}}$, which models surface tension effects (momentum exchange occurring across the fluid-fluid interface) as volume forces acting on the very small volume region used to describe the interface (a thin transition region between the two bulk fluids).

The function $\overline{\eta}(\phi,\lambda)$ in Eq.(6) is used to account for the non-uniform viscosity. In particular, assuming that the viscosity depends linearly on the order parameter ϕ (Kim (2012); Zheng *et al.* (2015)) we have:

$$\overline{\eta}(\phi,\lambda) = \frac{(\lambda-1)(\phi+1)}{2} \tag{11}$$

The governing equations are solved by a Fourier-Chebyshev pseudo-spectral method assuming no slip conditions at the channel walls. For the phase field ϕ, a zero-flux of the chemical potential and a fixed contact angle of $\pi/2$ *rad* are employed. These conditions lead to:

$$\mathbf{u}(z=\pm h) = \mathbf{0} \quad \frac{\partial \phi}{\partial z}(z=\pm h) = 0 \quad \frac{\partial^3 \phi}{\partial z^3}(z=\pm h) = 0 \tag{12}$$

Periodicity is applied for both $\mathbf{u}$ and ϕ in streamwise and spanwise directions (x and y). Note that the boundary conditions applied to ϕ direct imply the total conservation of the phase field over time, i.e $\frac{d}{dt}\int \phi dV = 0$.

The computational domain has dimensions $L_x \times L_y \times L_z = 4\pi h \times 2\pi h \times 2h$ and is discretized using $N_x \times N_y \times N_z = 512 \times 256 \times 257$ collocation points. As initial condition, we injected $N_0 = 256$ drops inside a fully developed turbulent channel flow at $Re_\tau = 150$. Drops are initially released on two different planes (128 drops for each plane) such that the center of mass of each drop is at 75 wall units from the wall. In wall units, the initial diameter of a drop is $D^+ = 90$, which gives a volume fraction of $\varphi = \frac{V_d}{V_d+V_c} = 0.183$, where V_c and V_d are respectively the volume of the continuous and of the dispersed phase (drops). To resolve the complex drops/turbulence interaction, the drops interface must be carefully described. In the present work, we use a minimum of three points to describe the interface (note that in the wall-normal direction, where the grid is finer, we use 5 to 7 grid points). Considering the constraint of having at least three points to describe the interface, we set $Ch = 0.0185$ and $Pe = 162.2$ (Magaletti *et al.* (2013); Yue *et al.* (2010)).

Simulations are run at a given Reynolds number ($Re_\tau = 150$) and assuming three different values of We: $We = 0.75$, $We = 1.5$ and $We = 3.0$. For each value of *We*, we consider five different values of the viscosity ratio λ: $\lambda = 0.01, \lambda = 0.1, \lambda = 1, \lambda = 10, \lambda = 100$. This gives a total of 15 simulations to cover the entire parameter range. Note that the value of Re_τ employed here is rather low, with the adopted grid making the simulations several time overresolved. However, due to the complexity represented by the multiphase flow description, the computational requirements are much larger than for a single phase simulation. An overview of the main simulations parameters is given in Tab. .

Sim	Re_τ	We	λ
S1	150	0.75	0.01
S2	150	0.75	0.10
S3	150	0.75	1.00
S4	150	0.75	10
S5	150	0.75	100
S6	150	1.50	0.01
S7	150	1.50	0.10
S8	150	1.50	1.00
S9	150	1.50	10
S10	150	1.50	100
S11	150	3.00	0.01
S12	150	3.00	0.10
S13	150	3.00	1.00
S14	150	3.00	10
S15	150	3.00	100

Table 1. Summary of the simulations perforemd

RESULTS

The dynamics of liquid drops immersed in a turbulent flow field is the result of a complex interaction between destabilizing actions due to shear and normal stresses at the drops interface and the stabilizing ones due to surface tension (which tends to preserve drop sphericity). Depending on the relative magnitude of destabilizing and stabilizing actions, drops deform, break and coalesce. When a viscosity difference between the liquid drops and the external fluid ($\lambda \neq 1$) exists, the picture becomes more complex and the internal viscosity of the drops (η_d) plays an active role in controlling the overall drops dynamics (Andersson & Andersson (2006); Cohen (1994)). In the following we will specifically focus on the role of surface tension (*We*) and viscosity ratio (λ) on the drops dynamics in a turbulent wall-bounded flow.

Influence of viscosity on the number of drops

When a swarm of liquid drops is injected in a turbulent liquid flow, simultaneous coalescence and breakup events are likely to occur (Shinnar (1961); Scarbolo *et al.* (2015)) with their balance ultimately determining the number of drops. To visualize the relative importance of these phenomena we therefore compute the time

behaviour of the number of drops $N(t)$ for the different cases considered. Results for $N(t)$ are shown in Fig. 1 and are normalized by the initial number of drops, N_0. Fig. 1(a), Fig. 1(b) and Fig. 1(c) refer to $We = 0.75$, $We = 1.5$ and $We = 3$ respectively. For each value of We, the drops behaviour for all the viscosity ratios ($\lambda = 0.01$, $\lambda = 0.10$, $\lambda = 1.00$, $\lambda = 10.0$ and $\lambda = 100$.) is considered. For $We = 0.75$, and regardless of the value of λ, $N(t)/N_0$ decreases monotonically in time. In particular, there is an initial stage (up to $t^+ \simeq 1000$) in which $N(t)/N_0$ decreases sharply in time, indicating a strong predominance of coalescence over breakup events with the consequent formation of few large drops. After this initial stage, the number of drops $N(t)/N_0$ achieves and almost constant value, which indeed barely depends on the value of λ; possibly we observe that the final number of drops, represented by the final plateau, is slightly larger for smaller λ. At this We, the large value of the surface tension compared to inertia hinders drops fragmentation (small deformability), even for small values of their internal viscosity. In Fig. 1(b) we observe the behaviour for $We = 1.5$: as expected, coalescence events dominate during the initial transient, and a statistically steady state is finally achieved in which the number of drops fluctuates around an average value. The effect of viscosity becomes larger in this case: for drops of small viscosity we observe a final number of drops which is about an order of magnitude bigger compared to the case in which the carrier fluid is less viscous than the drops. In Fig. 1(c) we can appreciate the role of drop viscosity at the highest We ($We = 3$). Drops coalescence dominates (i.e. the number of drops $N(t)/N_0$ decreases in time), until a critical drops size is attained, after which the number of drops achieves a plateau that does depend on λ. It is clear that when the drops viscosity is smaller than that of the carrier fluid ($\lambda < 1$), breakage is favoured. By contrast, when the drops viscosity is larger ($\lambda > 1$), coalescence is favoured. Of course, viscosity is not surface tension, and even if the effect of increasing drop viscosity (increasing λ) act as an increase of the surface tension (decrease of We), we must look for the physical mechanism which is ultimately related to turbulence modulation by viscosity. Lower values of the drops viscosity induce larger deformations that eventually cause drops fragmentation (i.e., small drops viscosity is a destabilizing factor). By contrast, large values of drops viscosity represent an extra stability factor for drops dynamics, which indeed induces smaller drops deformation and favours the occurrence of coalescence events. Only for $\lambda = 100$ the dynamics appears somehow different, with the initial transient decay extending up to $t^+ \simeq 800$ and an asymptotic condition characterized by a definitely smaller number of drops. However this represents an extreme case for which the stabilizing effect due to the large drops viscosity completely balances the small value of the surface tension, resulting in drops having an overall small deformability. A qualitative representation of the physical mechanism described above is given in Fig. 2-3 for the two limiting values of We: Fig. 2 refers to the case $We = 0.75$, whereas Fig. 3 refers to the case $We = 3$. For both $We = 0.75$ and $We = 3$, we show the drops dispersion and deformation in time (at three different time instants $t^+ = 300$, $t^+ = 600$ and $t^+ = 900$) for the two extreme cases $\lambda = 0.01$, Figs. 2-3(a)-(c), and $\lambda = 100$, Figs. 2-3(d)-(f). Together with the drops deformation, we also show the contour map of the Turbulent Kinetic Energy TKE, a quantity that may be related to drops deformation and dynamics. Note that $TKE = u_x'^2 + u_y'^2 + u_z'^2$ is shown on the channel center plane. In these figures, we observe that the number of drops reduces in time (time increases from (a) to (c)), regardless of the value of We and λ. For $We = 0.75$, the drops shape is rather smooth and slightly dependent on λ. However, for $We = 3$ (Fig. 3) the situation is remarkably different. The most striking feature observed in this case is the increased drop deformation and the formation of small drops fragments (particularly

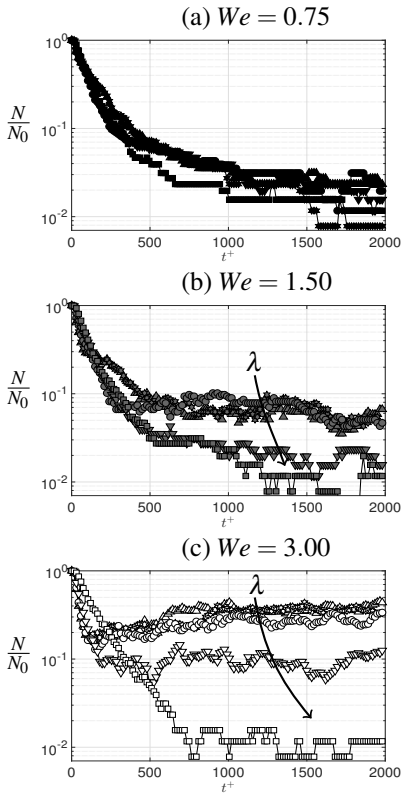

Figure 1. Time evolution of the normalized number of drops $N(t)/N_0$ for the three different values of We ($We = 075$, $We = 1.5$ and $We = 3$) considered in the present study. Panel (a) refers to $We = 0.75$, panel (b) to $We = 1.5$ and panel (c) to $We = 3$. In each panel, results for five different values of λ ($\lambda = 0.01$, $\lambda = 0.1$, $\lambda = 1$, $\lambda = 10$ and $\lambda = 100$) are shown. A sketch with the definition of λ and the color code is given beside each plot (right part of the figure).

for $\lambda = 0.01$), as a result of recurring and intensive breakup phenomena (Eastwood *et al.* (2004); Andersson & Andersson (2006)). From the underlying contour maps of TKE (shown in grayscale), we clearly identify the strong coupling between drops deformation and turbulence. Drops, which are first deformed by turbulence fluctuations, induce a turbulence modulation that is somehow linked to drops viscosity, size and deformation (which in turn depends on We and λ). In general, the larger is λ, the larger is the drops effect on the background turbulence.

CONCLUSIONS

Drops dynamics in turbulence is a complex phenomenon characterized by the competition between the destabilizing action of turbulence (which deforms and eventually brings the drops to breakage) and the stabilizing action of surface tension (which tends to preserve the drops integrity). When drops viscosity is different from that of the carrier fluid, the picture becomes even more complex since drops viscous dissipation can become important.

In this paper, we precisely focused on the complex interplay bewteen surface tension (We) and drop-to-fluid viscosity ratio (λ), which determines breakage and coalescence of large deformable drops in turbulence. Specifically, we studied the drops dynamics using Direct Numerical Simulations (DNS) of turbulence coupled with a Phase Field Model (PFM). We considered three different values of We ($We = 0.75$, $We = 1.5$ and $We = 3$), and five different values of λ ($\lambda = 0.01$, $\lambda = 0.10$, $\lambda = 1.00$, $\lambda = 10.0$ and $\lambda = 100$). For the base case $\lambda = 1$, we observed that drops dynamics is dom-

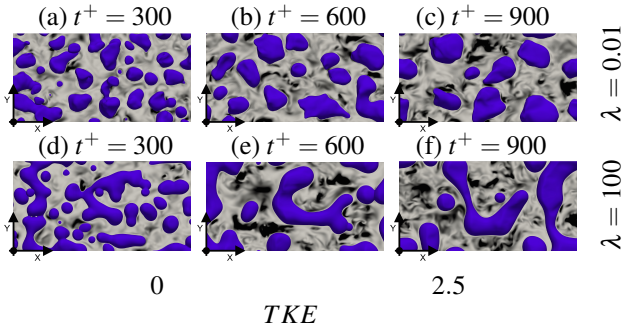

Figure 2. Drops evolution for $We = 0.75$ and for the two limiting cases $\lambda = 0.01$, panels (a)-(c) and $\lambda = 100$, panels (d)-(f). Each panel refers to a given time instant ($t^+ = 300$, $t^+ = 600$ and $t^+ = 900$). Contour maps of the Turbulent Kinetic Energy (TKE) computed on a plane passing through the channel center is also shown.

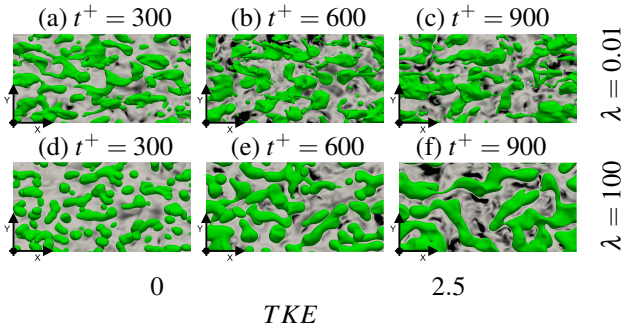

Figure 3. Drops evolution for $We = 3$ and for the two limiting cases $\lambda = 0.01$, panels (a)-(c) and $\lambda = 100$, panels (d)-(f). Each panel refers to a given time instant ($t^+ = 300$, $t^+ = 600$ and $t^+ = 900$). Contour maps of the Turbulent Kinetic Energy (TKE) computed on a plane passing through the channel center is also shown.

inated by coalescence for small We ($We < 1$), with breakup events entering the picture only for increasing We ($We > 1$). Interestingly, we found that this situation is selectively modified for $\lambda \neq 1$. For small We ($We < 1$), drops deformability remains small and the viscosity ratio λ does not influence the coalescence/breakup rate. For larger We ($We > 1$), drops deformability is increased and the viscosity ratio λ can significantly alter the coalescence and breakup dynamics. In particular, we observed that increasing drops viscosity reduces strongly the breakup rate (and increase the coalescence rate), very much like a reduction of We does. We linked this result to the increased value of the drops viscous dissipation which ultimately increases drops stability. Viscosity gradients across the interface of the drops act as modulators of the local shear stresses and can amplify or damp the inertial turbulence perturbations. Further analyses are required to examine the phenomena at larger values of drops to fluid viscosity ratios.

ACKNOWLEDGEMENTS

Support from EU FP7 Nugenia-Plus project (grant agreement No. 604965), from PRIN (under Grant 2006098584 004) and from Regione Autonoma Friuli Venezia Giulia under grant PAR FSC 2007/2013 are gratefully acknowledged. CINECA supercomputing center (Bologna, Italy) and ISCRA Computing Initiative are also gratefully acknowledged for generous allowance of computer resources.

REFERENCES

Ahmadi, S., Roccon, A., Zonta, F. & Soldati, A. in press Turbulent drag reduction in channel flow with viscosity stratified fluids. *Comput. Fluids* .

Anderson, D. M., McFadden, G. B. & Wheeler, A. A. 1998 Diffuse interface methods in fluid mechanics. *Annu. Rev. Fluid Mech.* **30** (1), 139–165.

Andersson, Ronnie & Andersson, Bengt 2006 On the breakup of fluid particles in turbulent flows. *AIChE J.* **52** (6), 2020–2030.

Ashgriz, N. & Poo, J. Y. 1990 Coalescence and separation in binary collisions of liquid drops. *J. Fluid Mech.* **221**, 183.

Badalassi, V. E., Ceniceros, H. D. & Banerjee, S. 2003 Computation of multiphase systems with phase field models. *J. Comput. Phys* **190** (2), 371–397.

Chen, H. T. & Middleman, S. 1967 Drop size distribution in agitated liquid-liquid systems. *AIChE J.* **13** (5), 989–995.

Chen, K., Bai, R. & Joseph, D. D. 1990 Lubricated pipelining. Part 3 Stability of core-annular flow in vertical pipes. *J. Fluid Mech.* **214**, 251–286.

Clay, P. H. 1940*a* The Mechanism of emulsion formation in turbulent flow Part I. *Proc.R.Acad.Sci* **43**.

Clay, P. H. 1940*b* The Mechanism of emulsion formation in turbulent flow Part II. *Proc.R.Acad.Sci* **43**.

Cohen, R. D. 1994 Brief communication. *Int. J. Multiph. Flow* **20** (1), 211–216.

Collins, S. B. & Knudsen, J. G. 1970 Drop-size distributions produced by turbulent pipe flow of immiscible liquids. *AIChE J.* **16** (6), 1072–1080.

Eastwood, C. D., Armi, L. & Lasheras, J. C. 2004 The breakup of immiscible fluids in turbulent flows. *J. Fluid Mech.* **502**, 309–333.

Hinze, J. O. 1955 Fundamentals of the hydrodynamic mechanism of splitting in dispersion processes. *AIChE J.* **1** (3), 289–295.

Howarth, W. J. 1964 Coalescence of drops in a turbulent flow field. *Chem. Eng. Sci.* **19** (1), 33 – 38.

Jacqmin, D. 1999 Calculation of Two-Phase Navier–Stokes Flows Using Phase-Field Modeling. *J. Comput. Phys* **155** (1), 96–127.

Joseph, D. D., Renardy, M. & Renardy, Y. 1984 Instability of the flow of two immiscible liquids with different viscosities in a pipe. *J. Fluid Mech.* **141**, 309–317.

Kim, J. 2012 Phase-Field Models for Multi-Component Fluid Flows. *Commun. Comput. Phys.* **12** (3), 613–661.

Komrakova, A. E., Eskin, D. & Derksen, J. J. 2015 Numerical study of turbulent liquid-liquid dispersions. *AIChE J.* **61** (8), 2618–2633.

Magaletti, F., Picano, F., Chinappi, M., Marino, L. & Casciola, C. M. 2013 The sharp-interface limit of the Cahn–Hilliard/Navier–Stokes model for binary fluids. *J. Fluid Mech.* **714**, 95–126.

Paulsen, J. D., Carmigniani, R. K., Kanman, A., Burton, J. C. & Nagel, S. R. 2014 Coalescence of bubbles and drops in an outer fluid. *Nat. Commun.* **5**, 3182.

Perlekar, P., Biferale, L. & Sbragaglia, M. 2012 Droplet size distribution in homogeneous isotropic turbulence. *Phys. Fluids* **065101**, 1–10.

Qian, D., McLaughlin, J. B., Sankaranarayanan, K., Sundaresan, S. & Kontomaris, K. 2006 Simulation of bubble breakup dynamics in homogeneous turbulence. *Chem. Eng. Commun.* **193** (8), 1038–1063.

Qian, J. & Law, C. K. 1997 Regimes of coalescence and separation in droplet collision. *J. Fluid Mech.* **331**, 59–80.

Scarbolo, L., Bianco, F. & Soldati, A. 2015 Coalescence and breakup of large droplets in turbulent channel flow. *Phys. Fluids* **27** (7), 073302.

Scarbolo, L., Molin, D., Perlekar, P., Sbragaglia, M., Soldati, A. & Toschi, F. 2013 Unified framework for a side-by-side comparison of different multicomponent algorithms: Lattice Boltzmann vs. phase field model. *J. Comput. Phys* **234**, 263–279.

Shinnar, R. 1961 On the behaviour of liquid dispersions in mixing vessels. *J. Fluid Mech.* **10** (02), 259.

Skartlien, R., Sollum, E. & Schumann, H. 2013 Droplet size distributions in turbulent emulsions: Breakup criteria and surfactant effects from direct numerical simulations. *J. Chem. Phys.* **139** (17).

Sleicher, C. A. 1962 Maximum stable drop size in turbulent flow. *AIChE J.* **8** (4), 471–477.

Wang, C. Y. & Calabrese, R. V. 1986*a* Drop breakup in turbulent stirred-tank contactors. Part II: Relative influence of viscosity and interfacial tension. *AIChE J.* **32** (4), 667–676.

Wang, C. Y. & Calabrese, R. V. 1986*b* Drop breakup in turbulent stirred-tank contactors. Part II: Relative influence of viscosity and interfacial tension. *AIChE J.* **32** (4), 667–676.

Wu, J., Lu, J., Wilson, C., Lin, Y. & Lu, H. 2010 Effective liquid-liquid extraction method for analysis of pyrethroid and phenylpyrazole pesticides in emulsion-prone surface water samples. *J. Chromatogr. A* **1217** (41), 6327–6333.

Yue, P., Feng, J., Liu, C. & Shen, J. 2004 A diffuse-interface method for simulating two-phase flows of complex fluids. *J. Fluid Mech.* **515**, 293–317.

Yue, P., Zhou, C. & Feng, James J. 2010 Sharp-interface limit of the Cahn–Hilliard model for moving contact lines. *J. Fluid Mech.* **645** (8), 279.

Zheng, X., Babaee, H., Dong, S., Chryssostomidis, C. & Karniadakis, G. E. 2015 A phase-field method for 3D simulation of two-phase heat transfer. *Int. J. Multiph. Flow* **82**, 282–298.